



This is a repository copy of *Roles of fibrin  $\alpha$ - and  $\gamma$ -chain specific cross-linking by FXIIIa in fibrin structure and function.*

White Rose Research Online URL for this paper:  
<http://eprints.whiterose.ac.uk/111563/>

Version: Accepted Version

---

**Article:**

Duval, C., Allan, P., Connell, S.D.A. et al. (3 more authors) (2014) Roles of fibrin  $\alpha$ - and  $\gamma$ -chain specific cross-linking by FXIIIa in fibrin structure and function. *Thrombosis and Haemostasis*, 111 (5). pp. 842-850. ISSN 0340-6245

<https://doi.org/10.1160/TH13-10-0855>

---

This article is not an exact copy of the original published article in *Thrombosis and Haemostasis*. The definitive publisher-authenticated version of C. Duval, P. Allan, S. D. A. Connell, V. C. Ridger, H. Philippou, R. A. S. Ariens, "Roles of fibrin  $\alpha$ - and  $\gamma$ -chain specific cross-linking by FXIIIa in fibrin structure and function", *Thrombosis and Haemostasis*, 2014: 111/5(May), pp. 781-1006 is available online at:  
<https://doi.org/10.1160/TH13-10-0855>.

**Reuse**

Unless indicated otherwise, fulltext items are protected by copyright with all rights reserved. The copyright exception in section 29 of the Copyright, Designs and Patents Act 1988 allows the making of a single copy solely for the purpose of non-commercial research or private study within the limits of fair dealing. The publisher or other rights-holder may allow further reproduction and re-use of this version - refer to the White Rose Research Online record for this item. Where records identify the publisher as the copyright holder, users can verify any specific terms of use on the publisher's website.

**Takedown**

If you consider content in White Rose Research Online to be in breach of UK law, please notify us by emailing [eprints@whiterose.ac.uk](mailto:eprints@whiterose.ac.uk) including the URL of the record and the reason for the withdrawal request.



[eprints@whiterose.ac.uk](mailto:eprints@whiterose.ac.uk)  
<https://eprints.whiterose.ac.uk/>

## **Roles of fibrin $\alpha$ - and $\gamma$ -chain specific cross-linking by FXIIIa in fibrin structure and function**

Cédric Duval<sup>1</sup>, Peter Allan<sup>1,2</sup>, Simon D.A. Connell<sup>2</sup>, Victoria C. Ridger<sup>3</sup>, Helen Philippou<sup>1</sup>, Robert A. S. Ariëns<sup>1</sup>.

<sup>1</sup> Theme Thrombosis, Division of Cardiovascular and Diabetes Research; Leeds Institute of Genetics, Health and Therapeutics; and Multidisciplinary Cardiovascular Research Centre; Faculty of Medicine and Health; University of Leeds; United Kingdom

+44(0)1133437734, C.Duval@leeds.ac.uk, phy3pa@gmail.com, H.Philippou@leeds.ac.uk, R.A.S.Ariens@leeds.ac.uk

<sup>2</sup> Molecular and Nanoscale Physics Group, School of Physics and Astronomy, University of Leeds, United Kingdom

+44(0)1133438241, S.D.A.CConnell@leeds.ac.uk

<sup>3</sup> Department of Cardiovascular Science; Faculty of Medicine, Dentistry, and Health; University of Sheffield; United Kingdom

+44(0)1142261410, V.C.Ridger@sheffield.ac.uk

**Short Running Title:** Roles of  $\alpha$ - and  $\gamma$ -crosslinking in fibrin structure

**Correspondence:** Robert A. S. Ariëns, Theme Thrombosis; Division of Cardiovascular and Diabetes Research; Leeds Institute of genetics, Health, and Therapeutics; Clarendon Way; University of Leeds; LS2 9NL; United Kingdom. Tel: +44(0)1133437734. Email: R.A.S.Ariens@leeds.ac.uk

**Category:** Original article - Blood coagulation, fibrinolysis and cellular haemostasis.

**Keywords:** Fibrinogen, factor XIII, clot structure.

**Abbreviations:** Fbg, Fibrinogen; FXIIIa, Activated factor XIII;  $G'$ , Storage modulus;  $G''$ , Loss modulus; OD, Optical density;  $\tan\delta$ , Loss tangent; TBS, Tris buffered saline; tPA, Tissue plasminogen activator; 3X, Triple mutant; WT, Wild-type.

**Manuscript word count (w/o reference, figure legends, tables):** 4526.

### **Funding**

This study was supported by Medical Research Council (G0901546) and British Heart Foundation (RG/13/2/30104) grants.

## **SUMMARY**

Factor XIII is responsible for the cross-linking of fibrin  $\gamma$ -chains in the early stages of clot formation, whilst  $\alpha$ -chain cross-linking occurs at a slower rate. Although  $\gamma$ - and  $\alpha$ -chain cross-linking was previously shown to contribute to clot stiffness, the role of cross-linking of both chains in determining clot structure is currently unknown. Therefore, the aim of this study was to determine the role of individual  $\alpha$ - and  $\gamma$ -chain cross-linking during clot formation, and its effects on clot structure.

We made use of a recombinant fibrinogen ( $\gamma$ Q398N/Q399N/K406R), which does not allow for  $\gamma$ -chain cross-linking. In the absence of cross-linking, intact D-D interface was shown to play a potential role in fiber appearance time, clot stiffness and elasticity. Cross-linking of the fibrin  $\alpha$ -chain played a role in the thickening of the fibrin fibers over time, and decreased lysis rate in the absence of  $\alpha$ 2-antiplasmin. We also showed that  $\alpha$ -chain cross-linking played a role in the timing of fiber appearance, straightening fibers, increasing clot stiffness and reducing clot deformation. Cross-linking of the  $\gamma$ -chain played a role in fibrin fiber appearance time and fiber density.

Our results show that  $\alpha$ - and  $\gamma$ -chain cross-linking play independent and specific roles in fibrin clot formation and structure.

Word count: 200

## **INTRODUCTION**

Formation of a cross-linked fibrin clot is central to hemostasis and thrombosis. Upon clot formation, activated factor XIII (FXIIIa) produces  $\gamma$ -glutamyl- $\epsilon$ -lysine isopeptide bonds between two fibrin molecules within the fibrin fiber assembly, increasing clot stiffness<sup>1</sup>. FXIIIa cross-links the fibrin  $\alpha$ - and  $\gamma$ -chains of fibrin. This cross-linking occurs at different rates, whereby the  $\gamma$ -chains are more rapidly cross-linked between residues  $\gamma$ Q398 and/or  $\gamma$ Q399 and  $\gamma$ K406<sup>2,3</sup>. Cross-linking of the  $\alpha$ -chains occurs at a much slower rate between  $\alpha$ Q221,  $\alpha$ Q237,  $\alpha$ Q328,  $\alpha$ Q366 and numerous lysine residues<sup>4,5,6</sup>.

FXIIIa cross-linking has been shown to alter the viscoelastic properties of fibrin clots<sup>7-10</sup>, but the effects of cross-linking on the structure of fibrin clots is still poorly understood. Two previous reports indirectly suggested that FXIIIa may also influence the structure of clots. Ryan et al. reported that the average fiber diameter decreased after cross-linking by FXIIIa<sup>9</sup>. We previously found that a FXIII-A (A-subunit) genetic polymorphism, V34L, where Leu34 was activated twice as fast as Val34, influenced clot structure whereby FXIII-A Leu34 resulted in a clot with thinner fibers and smaller pores<sup>11</sup>. However, the direct effects of FXIII cross-linking on fibrin fiber and network ultrastructure have hitherto not been investigated and the mechanisms by which these changes occur are also unknown.

The structure of the fibrin clot has repeatedly been shown to be abnormal in patients with venous and arterial thrombosis, and to play important roles in the regulation of the mechanical properties of the clot and its resistance to fibrinolysis (for a review, see Undas & Ariëns<sup>12</sup>). Therefore, the modification of fibrin fiber and network structure by FXIIIa could provide an important new mechanism by which FXIIIa influences thrombosis. We have developed a recombinant fibrinogen with mutations in the  $\gamma$ -chain cross-linking sites for FXIIIa (fibrinogen  $\gamma$ Q<sub>398</sub>N/Q<sub>399</sub>N/K<sub>406</sub>R, 3X, or triple-mutant)<sup>13</sup> to directly investigate the role of cross-linking in fibrin clot structure and function. We find that cross-linking by FXIIIa does not merely stabilize an already existing fibrin clot structure, but that it directly influences the ultrastructure of the fibrin

fiber network. We also find that cross-linking of the  $\gamma$ - and  $\alpha$ -chains is responsible for these effects, and that they play specific and complementary roles in this process.

## **MATERIALS AND METHODS**

### **Materials**

Human  $\alpha$ -thrombin (Calbiochem; Nottingham, UK) was reconstituted to 250U/mL, tissue plasminogen activator (tPA; Pathway Diagnostics; Dorking, UK) and Glu-plasminogen (ERL; Swansea, UK) were diluted in 0.05 M Tris-HCl, 0.1M NaCl, pH7.4 (TBS) to 14nM and 11 $\mu$ M respectively, and stored at -80°C. Human FXIII-A<sub>2</sub>B<sub>2</sub> was isolated from contaminating albumin and glucose from Fibrogammin P (CSL Behring; Haywards Heath, UK) by Sepharose-6B gel filtration as described previously<sup>13</sup>. FXIII was diluted in TBS to 110 $\mu$ g/mL and stored at -80°C. AlexaFluor488 fibrinogen (Invitrogen; Paisley, UK) was diluted in TBS to 2mg/mL and stored at -80°C. All other chemicals were obtained from Sigma (Gillingham, UK) unless stated otherwise.

### **Fibrinogen expression**

Recombinant human  $\gamma$ Q<sub>398</sub>N/Q<sub>399</sub>N/K<sub>406</sub>R (3X) fibrinogen was prepared as previously described<sup>13</sup>. In brief, the expression vector containing the full  $\gamma$ -chain cDNA (pMLP- $\gamma$ ) was mutated at codons 398, 399 and 406 using QuickChange site-directed mutagenesis kit (Agilent Technologies; Stockport, UK). Chinese hamster ovary (CHO) cells, already containing the human A $\alpha$  and B $\beta$  chains were co-transfected with the mutated pMLP- $\gamma$  and pMSV-His (selection vector). CHO cells expressing either human wild-type fibrinogen, or the 3X fibrinogen, were grown in Petri dishes, and transferred into roller bottles containing adherent microcarrier beads and DMEM F12 medium (Invitrogen) supplemented with 2mg/mL aprotinin and 5mg/mL insulin, transferrin sodium selenite supplement (Roche; Burgess Hill, UK). The medium was harvested and replaced every 48hrs, and stored at -80°C in the presence of 150 $\mu$ M PMSF. Medium was harvested for as long as fibrinogen was detectable by ELISA. Fibrinogen was precipitated overnight with 40% saturated ammonium sulphate (Fisher Scientific; Loughborough, UK) and purified, as previously described<sup>14</sup>, with the following modifications: a) 50mM Tris-HCl (pH7.6) and 100mM NaCl were replaced by 20mM MES (pH5.6) in the 40x buffer. b) 10U/mL aprotinin was replaced by 10U/mL soybean trypsin inhibitor in the buffer A1. c) Protamine / sepharose chromatography was replaced by IF-1 mAb (10mg; Kamiya Biomedical; Seattle, USA)<sup>15</sup> / sepharose (1.5mg; VWR; Lutterworth, UK) immunoaffinity chromatography.

Prior to chromatography, CaCl<sub>2</sub> was added to the samples (10mM final). The fibrinogens were eluted in TBS containing 5mM EDTA, and dialysed overnight against TBS. The concentration and purity of the fibrinogen preparations were determined at A<sub>280nm</sub> (extinction coefficient 15.1 for a 1mg/mL fibrinogen solution with a 1cm path length at 280nm) and by SDS-PAGE in reducing conditions, respectively.

### **Turbidity analysis of fibrin polymerization**

Polymerization of fibrin was studied by turbidity analysis as described<sup>16</sup>. In brief, fibrinogen (0.5mg/mL), CaCl<sub>2</sub> (5mM) and FXIII (3.7μg/mL) were diluted in TBS and premixed in 96-well plates in triplicate. Thrombin (0.1U/mL final concentration) was added to initiate clotting, and absorbency was measured at 340nm, every 12s for 2hrs at room temperature, using a BioTek ELX808 microtiter plate reader (Labtech International; Ringmer, UK). Experiments were performed in triplicate.

### **Fibrinolysis analysis by turbidity**

Fibrin clot lysis was studied using an adapted turbidity assay (above) in which tPA and plasminogen were included in the reaction mixture. Fibrinogen (0.5mg/mL), CaCl<sub>2</sub> (5mM), tPA (100pM), Glu-plasminogen (0.24μM) and FXIII (3.7μg/mL) were diluted in TBS and premixed in 96-well plates in triplicate. Thrombin (0.1U/mL final concentration) was added to initiate clotting, and changes in absorbency were monitored at 340nm, every 12s for 2hrs at room temperature, using a BioTek ELX808 microtiter plate reader (Labtech International; Ringmer, UK). Experiments were performed in triplicate. Lysis rates were calculated by determining the slope of a straight line drawn through the polymerization curve at the point of its steepest inclination. Lysis rate were expressed as change in optical density per second ( $\Delta$  OD/s).

### **Laser Scanning Confocal Microscopy**

Fibrinogen (0.5mg/mL), CaCl<sub>2</sub> (5mM), AlexaFluor488 fibrinogen (1% w/w) and FXIII (3.7μg/mL) were diluted in TBS. After addition of thrombin (0.1U/mL final concentration), the reaction mixture was transferred into the channel of an uncoated Ibidi μ-slide VI (Thistle Scientific; Glasgow, UK), before being immediately observed by laser scanning confocal microscopy (LSCM). Imaging was performed using an

upright Zeiss LSM-510 META Axioplan2 microscope (Carl Zeiss; Welwyn Garden City, UK) with a 63x oil immersion objective lens. Optical z-stacks were obtained, every 2 $\mu$ m over 20 $\mu$ m, and combined into single projected images. Fiber density was determined by counting the number of fibers crossing an arbitrary line of fixed length (200 $\mu$ m) drawn through a single optical section. Each fibrin clot was prepared in duplicate and three density measurements were performed in each.

### **Field Emission Scanning Electron Microscopy**

Fibrinogen (0.5mg/mL), CaCl<sub>2</sub> (5mM), FXIII (3.7 $\mu$ g/mL) were premixed in TBS, before adding thrombin (0.1U/mL). The reaction mix (50 $\mu$ L) was transferred into pierced Eppendorf lids, to allow fixing and washing of the clot. Clots were left to form in a humidity chamber for 1hr at room temperature, before being washed with sodium cacodylate buffer (67mM, pH7.4) to remove excess salt. Clots were then fixed overnight in 2% glutaraldehyde, and further washed in sodium cacodylate buffer, before being dehydrated in a series of increasing acetone concentrations (30-100%). Critical-point drying with CO<sub>2</sub>, mounting onto stubs, sputter-coating with platinum using a Cressington 208 HR (Cressington Scientific Instruments; Watford, UK), were then performed before imaging the clots using a FEI Quanta 200 FEGSEM (FEI; Hillsboro, USA).

### **Fibrin viscoelastic properties**

We measured the viscoelastic properties of fibrin clots using a magnetic microrheometer device as previously described<sup>17</sup>. Fibrinogen (0.5mg/mL), CaCl<sub>2</sub> (5mM), and FXIII (3.7 $\mu$ g/mL) were diluted in TBS. After the addition of paramagnetic particles (4.5 $\mu$ m diameter; Dynal; Oslo, Norway) and thrombin (0.1U/mL), the reaction mixture was transferred into 500 $\mu$ m diameter capillaries (VitroCom, Mountain Lakes, USA). Once filled, the capillary ends were sealed with Vaseline, and the clots were left to form overnight. Clot viscoelastic properties were measured using a magnetic microrheometer, as previously described<sup>18</sup>. Clot stiffness (storage modulus, G') and viscosity (loss modulus, G'') were calculated as previously described<sup>19</sup>. The ratio of energy dissipated to energy stored (loss tangent,  $\tan\delta = G''/G'$ ), which reflects clot stability was also calculated<sup>10</sup>. Measurements were repeated for 10 particles per clot, in triplicate.

**Data analysis**

All data are presented as mean $\pm$ SEM, and all statistical analysis (t-test) were performed using GraphPad. P-values of lower than 0.05 were considered to indicate statistical significance.

## **RESULTS**

### **The effect of cross-linking by FXIII on fibrin polymerisation**

Turbidity analysis showed a small but significant difference in polymerization patterns between wild-type (WT) and triple-mutant (3X) fibrinogens (Figure 1). Although polymerization rates and time to reach plateau were similar in either fibrinogen in the absence of cross-linking by FXIIIa, maximum optical density (Max OD) was significantly higher ( $p < 0.05$ ) in WT (1.33-fold) compared to that of 3X, indicating that the triple mutant fibrinogen produced clots with thinner fibres and increased fiber density. While this indicated that the mutations in the 3X fibrinogen were directly responsible for minor changes in fibrin polymerization and the structure of the fibrin network, these results did not preclude the use of the 3X and WT fibrinogen to study the effects of cross-linking by FXIIIa on clot structure. When FXIII was added prior to clot formation, a similar significant increase ( $p < 0.05$ ) in Max OD was observed for both WT (1.21) and 3X (1.18) fibrinogens, indicating that in both cases addition of FXIII leads to clots with thicker fibers. Although the initial polymerization rates were unchanged, the time to reach Max OD at a later stage was significantly lengthened ( $p < 0.001$ ) by the addition of FXIII, from 25min to 69min and 30min to 64min for WT and 3X fibrinogens respectively. These data suggest that once polymerization by thrombin alone is complete, cross-linking by FXIIIa continues to affect clot structure, by increasing fiber thickness over time. Furthermore, since Max OD increased in both WT and 3X fibrinogen (the latter of which does not support  $\gamma$ -chain crosslinking), these data show that the late changes in fibrin structure are due to cross-linking of the  $\alpha$ -chains.

### **Cross-linking by FXIIIa reduces fibrinolysis rates**

Turbidity analysis showed a difference in lysis between WT and 3X fibrinogens (Figure 2). Similar to the data obtained in the absence of tPA and plasminogen, Max OD was reduced for clots made with 3X compared with WT fibrinogen. In the absence of FXIII, lysis rates were similar for clots made from both WT ( $-2.30 \times 10^{-4}$  unit/sec) and 3X ( $-2.32 \times 10^{-4}$  unit/sec) fibrinogens. These rates were significantly decreased when FXIII was added, both WT ( $-1.97 \times 10^{-4}$  Unit/sec) and 3X ( $-1.96 \times 10^{-4}$ )

fibrinogens showed a similar decrease (1.18- and 1.17-fold respectively,  $p < 0.05$ ). When lysis rates were normalized to the maximum absorbency of each data set, the decrease in lysis rates after cross-linking by FXIIIa was further accentuated to 1.26- and 1.29-fold for clots made with WT- and 3X-fibrinogen, respectively. In addition, when FXIII was added, the time to half-lysis was significantly prolonged by 1.23- and 1.16-fold ( $p < 0.05$ ) for WT- and 3X-fibrinogen, respectively. These data, which were obtained using purified proteins and recombinant fibrinogen, in the absence of  $\alpha_2$ -antiplasmin, show that cross-linking by FXIIIa decreases lysis rate independently of other plasma proteins, and that this effect is mainly due to cross-linking of the  $\alpha$ -chains.

### **Effects of cross-linking on fiber density and fiber appearance times**

In agreement with the turbidity results, laser scanning confocal microscopy showed that after 60min, in the absence of FXIII, clots formed with 3X fibrinogen were significantly denser, than those formed with WT fibrinogen (Figs. 3A, 3C, and 3E). When FXIII was added, the fiber density was significantly increased for WT but not 3X fibrinogen (Figs. 3B, 3D, and 3E). These data suggest that  $\gamma$ -chain rather than  $\alpha$ -chain cross-linking influences fiber density. When images were captured every 30sec throughout the clot formation, in the absence of FXIII, fibers appeared after 3.0min and 3.5min for fibrinogen WT and 3X respectively (Supplementary Figure). When FXIII was added, WT and 3X fibers were first observed 30sec earlier, at 2.5min and 3.0min respectively (Supplementary Figure). This phenomenon was also observed when the turbidity data were zoomed in for the first 3 minutes. The order of length of time required to reach a determined OD (Figure 1 inset) correlated with that of the visual appearance of the fibers. These data suggest that intact  $\gamma$ -chain plays a role in fiber appearance time, along with  $\alpha$ -chain cross-linking.

### **Cross-linking by FXIIIa straightens fibers**

Electron microscopy analysis of clots formed in the absence of FXIII showed no major difference for fibrinogen 3X compared to fibrinogen WT (Figs. 4C and 4A, respectively). However, it was striking to observe that for both fibrinogens (Figs. 4B and 4D) the fibers appeared to be straighter compared with those produced in the absence of FXIII (Figs. 4A and 4C, respectively). In the absence of FXIII, fibrin fibers

exhibited greater curvature, and the effect of straightening of the fibers occurred after the addition of FXIII to clots made from both WT and 3X fibrinogen, indicating that  $\alpha$ -chain cross-linking plays a role in fiber straightness in electron microscopy.

### **Cross-linking by FXIIIa increases clot stiffness and decreases clot deformation**

The viscoelastic properties of clots were measured using a magnetic microrheometer (Figure 5). In the absence of FXIII, clots formed with fibrinogen WT were significantly stiffer ( $p < 0.05$ ) compared to fibrinogen 3X, as indicated by the 1.5-fold higher storage modulus  $G'$  (Figure 5A). The loss modulus  $G''$  was significantly higher (2-fold,  $p < 0.005$ ), in clots formed with fibrinogen 3X compared to fibrinogen WT (Figure 5B), indicating that 3X clots are more susceptible to inelastic deformation. The storage modulus reflects the elastic energy stored by the clot during deformation, whilst the loss modulus reflects the viscous properties of the clot, i.e. its permanent inelastic deformability. When FXIII was added, stiffness was significantly increased for clots formed by both WT (1.3-fold,  $p < 0.01$ ), and 3X (1.4-fold,  $p < 0.05$ ) fibrinogen (Figure 5A). Similarly, the loss modulus was significantly decreased by fiber cross-linking in clots formed by WT (1.5-fold,  $p < 0.005$ ) and 3X (1.4-fold,  $p < 0.01$ ) fibrinogens (Figure 5B). The loss tangent,  $\tan\delta$  relates to the overall plastic stability of the clot. In the absence of cross-linking,  $\tan\delta$  was significantly higher (2.6-fold,  $p < 0.05$ ) in 3X clots compared to the WT clots, indicating that the latter are more stable and less susceptible to permanent deformation. In the presence of FXIII,  $\tan\delta$  was decreased for both WT (1.7-fold) and 3X (2.4-fold) clots (Figure 5C). These results indicate that  $\alpha$ -chain cross-linking plays a role in increasing clot stiffness and plastic stability, and decreasing clot inelastic deformation.

## **DISCUSSION**

Our study provides novel evidence that cross-linking of the  $\alpha$ - and  $\gamma$ -chains of fibrin by FXIIIa plays a direct role in the regulation of fibrin clot ultrastructure. Using recombinant wild-type fibrinogen and fibrinogen with mutations in the  $\gamma$ -chain cross-linking sites we show that cross-linking by FXIIIa influences fibrin clot formation and structure. We find that cross-linking of the fibrin  $\alpha$ -chains by FXIIIa influences fibrin polymerization long after the effects of thrombin have worn off. We also find that  $\alpha$ -chain cross-linking directly influences fibrinolysis rates and decreases fibrin fiber curvature observed by electron microscopy, whereas cross-linking of the  $\gamma$ -chains influences fiber density. Fibrin microrheological properties are mostly regulated by  $\alpha$ -chain cross-linking. These data demonstrate that cross-linking by FXIIIa influences fibrin formation, clot structure, and its stability, and that  $\alpha$ - and  $\gamma$ -chain cross-linking play specific and complementary roles in these processes. In view of the role of fibrin structure in thrombosis<sup>12</sup>, these findings indicate a novel role for FXIIIa in regulating thrombosis.

We investigated the characteristics of the clot during its formation, but also its structure once formed, in a variant fibrinogen that does not form  $\gamma$ - $\gamma$  cross-links. During the polymerization process, minor differences were observed between WT and 3X fibrinogens with regards to polymerization onset and maximum absorbency. In the absence of cross-linking, we found that visually (confocal microscopy) the fibers appeared later in the case of fibrinogen 3X compared to WT. This was also observed when analyzing the early stages of polymerization by turbidity, therefore we hypothesize that this phenomenon may be due to impaired protofibril formation, resulting in a delayed lateral aggregation, and therefore fiber appearance, although the rate of polymerization was not apparently altered. Although the mutations produced in fibrinogen 3X ( $\gamma$ Q398N/Q399N/K406R) were selected on the basis that the new amino-acids show similar chemical and structural characteristics, this impaired protofibril formation could be caused by these mutations, as it was suggested that  $\gamma$ -dimerization occurs as soon as the fibrin molecules associate<sup>20</sup>. Residue  $\gamma$ Q398 was shown to be located on the edge of the D-D interface by X-ray crystallography<sup>21</sup>, which would make this residue, and residue  $\gamma$ Q399, more readily

accessible to FXIIIa for cross-linking. This location at the edge of the D-D interface suggests that a mutation at this site may induce small alterations to the area involved in D-D interactions. The exact location of  $\gamma$ K406 with regards to the D-D interface is unresolved in the crystal structure, but its close proximity to  $\gamma$ Q398 would indicate that it could also interfere with D-D interactions and protofibril formation. A somewhat larger change in amino acid characteristics is observed for the substitution of lysine with arginine ( $\gamma$ K406R), where 2 amine groups are added due to the mutagenesis, which could trigger a slight change in conformation, hence affecting polymerization. No naturally occurring mutations of these amino acids have been documented. Further analysis of the role of these particular residues in D-D interactions requires characterization of the D-D interface for fibrinogen 3X and WT by crystallography in a future study.

When polymerization occurred in the absence of cross-linking, turbidity and confocal data showed that fibrinogen 3X formed denser clots compared to WT fibrinogen. In the presence of FXIIIa, it was observed that upon completion of polymerization, absorbency continued to increase for both fibrinogens for over an hour. Since  $\alpha$ -chain cross-linking occurs over a similar time span, and lateral aggregation likely involves  $\alpha$ - $\alpha$  interactions<sup>22</sup> these data indicate that  $\alpha$ -chain cross-linking plays a role in fiber thickening once the initial phase of polymerization is complete. It is possible that  $\alpha$ -chain cross-linking plays a role in the continued remodeling of the clot, as recently described by Chernysh et al.<sup>23</sup>. Cross-linking of the  $\gamma$ -chain appears to play a significant role in determining the fiber density, as an increase was observed when FXIIIa was added to fibrinogen WT which was not present in the case of fibrinogen 3X. We hypothesize that during clot formation,  $\gamma$ -chain cross-linking may help to stabilize branching of fibers<sup>24</sup>, leading to an increase in fiber density. These data are in agreement with Carlisle et al., who found that cross-linking of fibrin by FXIIIa particularly increased the resistance of fiber branchpoints to rupture during pulling experiments with the atomic force microscope<sup>25</sup>. In the absence of cross-linking fiber branching may prove less stable, and therefore a reduction in the number of stable branchpoints in the absence of cross-linking by FXIIIa could lead to clots with a lower fiber density, since fiber density is determined as the number of fibers between branchpoints in a certain area (or over a certain length) of the clot.

Turbidity analysis to determine the functional relevance of the individual chain cross-linking on fibrinolysis showed that in the absence of  $\alpha$ 2-antiplasmin, cross-linking of the  $\alpha$ -chain is responsible for a decrease in fibrinolysis rate. A previous study has shown that FXIIIa cross-linking increased clots resistance to lysis<sup>26</sup>, however this study was performed with plasma and plasma-purified proteins. Our study uses recombinant proteins which are not subject to possible contamination with other plasma proteins ( $\alpha$ 2-antiplasmin in particular), showing that this effect is directly FXIIIa-dependent. The apparent role of the  $\alpha$ -chain in this process could be due to the number of cross-linking sites present on this chain, which is far more compared to that of the  $\gamma$ -chain. In addition, since inter-protofibril cross-links (produced in the  $\alpha$ -chains) are present in greater number than intra-protofibril cross-links (produced in the  $\gamma$ -chain), more cleavages by plasmin are required to dissolve the network. Our data therefore show that  $\alpha$ -chain cross-linking reduces susceptibility of the fibrin network to fibrinolysis to a certain degree directly, although we recognize that incorporation of  $\alpha$ 2-antiplasmin by FXIIIa into Lys303 of the fibrin  $\alpha$ -chain has a much larger effect on the resistance of the clot to fibrinolysis as previously demonstrated by Fraser et al..<sup>27</sup>. Future studies using recombinant fibrinogen with mutations in the cross-linking site for  $\alpha$ 2-antiplasmin will be required to shed further light on the roles of  $\alpha$ 2-antiplasmin dependent and independent effects on fibrinolysis.

We found that when the viscoelastic properties of clots were investigated using a magnetic microrheometer, clots made with fibrinogen WT showed a significantly higher stiffness (storage modulus or G') compared to those made with fibrinogen 3X. Cross-linking of these fibrinogens by FXIIIa resulted in a further significant increase in clot stiffness which was similar for both fibrinogens, indicating that the increased stiffness upon cross-linking is largely dependent on the  $\alpha$ -chains. Previous studies have found that cross-linking by FXIIIa resulted in clots with increased stiffness and reduced inelastic deformation<sup>8,9,20</sup>. Furthermore, a previous study using a recombinant fibrinogen truncated at A $\alpha$ 251 and therefore lacking most of the  $\alpha$ -chain cross-linking sites, also found that cross-linking of the  $\alpha$ -chain plays a major role in the determination of fibrin stiffness, since the storage modulus of clots made with this variant was significantly reduced compared to clots made from WT fibrinogen.<sup>22</sup> Our

current findings using a mutant that lacks all three  $\gamma$ -chain cross-linking sites, extend these data and confirm that  $\alpha$ -chain cross-linking plays a major role in clot stiffness. In previous reports, we made similar observations using the 3X fibrinogen variant in bulk measurements of fibrin clots<sup>13</sup> and also at the single fiber level<sup>28</sup>, although in these studies a smaller increase in stiffness with fibrinogen 3X cross-linking compared to fibrinogen WT was observed, indicating a role also for  $\gamma$ -chain cross-linking in fibrin stiffness. The reasons for the apparent discrepancies with regards to the role of  $\gamma$ -chain cross-linking in fibrin stiffness between the current study and these earlier studies are unclear, but could involve differences in fibrin formation conditions and differences in the measurement techniques employed. In the current study we studied the rheological properties at a micron scale level of a paramagnetic bead with a diameter of 4.5 $\mu$ m trapped by a number of fibrin fibers (magnetic microrheometer), as opposed to the whole clot rheology using a torsion pendulum and the single fiber mechanical properties investigated by atomic force microscopy in our previous studies<sup>13,28</sup>. It appears that under the conditions used in the current study, cross-linking of the  $\gamma$ -chains plays a smaller role in determining fibrin stiffness as compared to that of the  $\alpha$ -chains.

Loss modulus ( $G''$ ) was also measured, and we found that clots produced with fibrinogen 3X were more susceptible to inelastic deformation compared to fibrinogen WT. Upon cross-linking, clots made of both fibrinogens showed a decrease in inelastic deformation as the clots stiffened, indicating that the cross-linking dependent increase in clot stiffness is  $\alpha$ -chain dependent. This observation is in agreement with the observations made at the single fiber level<sup>28</sup>. The overall clot plastic stability (loss tangent) was determined from the storage and loss moduli, and clots formed from 3X fibrinogen showed an intrinsic decrease in plastic stability compared to WT fibrinogen. In the presence of cross-linking this plastic stability was increased for clots made of both fibrinogen variants, indicating that this effect is largely  $\alpha$ -chain dependent.

Previous studies have shown that the storage modulus ( $G'$ ) directly relates to the density of cross-links in a clot<sup>20</sup>, in particular  $\alpha$ -chain cross-links. The authors hypothesized that this is due to the larger amount of cross-linking sites in the  $\alpha$ -chain,

compared to  $\gamma$ -chain. Our current study is in agreement with this, since no major difference was observed in the level of increase of clot stiffness upon cross-linking in clots made from WT and 3X fibrinogens.

Electron microscopy analysis of clots formed with both fibrinogens, in the absence and presence of FXIIIa, provided additional insights into the effects of cross-linking by FXIIIa on fibrin clot structure and fiber tautness. In the absence of cross-linking, both fibrinogens formed similar clots with regards to fiber curvature. Interestingly, in the presence of cross-linking by FXIIIa, both sets of fibrinogens produced clots with much straighter fibers, indicating that  $\alpha$ -chain cross-linking plays a role in reducing fiber curvature. The reduction of fiber curvature following cross-linking by FXIIIa is likely caused by the increase in fiber stiffness, and decrease in inelastic deformation of the fibers. It may be possible that the curvature observed in the absence of FXIIIa is due to the sample preparation procedures used prior to imaging the clot, which include fixation, dehydration and critical point drying. This was further supported by the absence of difference in fibers curvature, before and after cross-linking, in fully hydrated clots observed by confocal microscopy. However, the absence of such curvature following cross-linking is an indication that  $\alpha$ -chain cross-linking may protect the fibrin fibers against this inelastic deformation. The  $\alpha$ - $\alpha$  cross-links introduced by FXIIIa in the fibrin fiber assembly likely result in more rigid and taut fibers, which could be less prone to bending and remain tense, even during dehydration and critical point drying of the clots as required for imaging by the electron microscope. Sample preparation for electron microscopy may also partly explain the apparent discrepancies between the electron microscopy and turbidity observations. Although turbidity indicated that WT fibrinogen produced clots with thicker fibers than 3X fibrinogen in the absence of FXIIIa, and that cross-linking increased fiber thickness in clots made from either fibrinogen, no major differences in fiber diameters were observed by electron microscopy, possibly due to effects of sample dehydration on fiber thickness in these experiments.

Fibrin clot formation is a highly dynamic process whereby cross-linking of the fibrin fibers by FXIIIa occurs whilst the network is still being formed. Our study through the use of recombinant fibrinogens with mutations in the FXIII cross-linking sites presents

novel, direct data demonstrating that cross-linking by FXIIIa, or the absence of it, plays an important role in the final structure and function of the clot. In addition, we have found that cross-linking of the fibrin  $\alpha$ - and  $\gamma$ -chains play different, specific and complementary roles during clot formation (Table 1), ultimately each impacting on particular aspects of fibrin clot structure and function. These data show that cross-linking by FXIIIa does not merely stabilize an already existing fibrin network structure but influences its formation and structure. Our findings have important implications for the understanding of the molecular processes involved in clot formation and stability.

### **WHAT IS KNOWN ABOUT THIS TOPIC?**

- Activated factor XIII cross-links the fibrin  $\alpha$ - and  $\gamma$ -chains.
- Cross-linking by activated factor XIII increases stiffness of the fibrin clots, and resistance of the clot to fibrinolysis by incorporation of  $\alpha$ 2-antiplasmin.
- A functional genetic polymorphism in factor XIII (Val34Leu) has been associated with changes in clot structure.

### **WHAT DOES THIS PAPER ADD?**

- Recombinant fibrinogens with mutations in the cross-linking sites show that activated factor XIII does not stabilize an already existing fibrin clot structure but directly modulates fibrin formation and network structure.
- Cross-linking of the fibrin  $\alpha$ - and  $\gamma$ -chains play specific and complementary roles in modulating fibrin clot structure.
- Cross-linking of the fibrin  $\alpha$ -chain by activated factor XIII reduces fibrinolysis rate independently of  $\alpha$ 2-antiplasmin.

## **AUTHORS CONTRIBUTIONS**

C. Duval performed research, analysed data, wrote the paper. P. Allan performed research. S.D.A. Connell, V.C. Ridger and H. Philippou designed research. R.A.S. Ariens designed research, wrote the paper. All authors have contributed to revision of the manuscript.

## **CONFLICTS OF INTEREST**

None declared.

## **REFERENCES**

1. Lorand L. Factor XIII: structure, activation, and interactions with fibrinogen and fibrin. *Ann N Y Acad Sci* 2001;936:291-311.
2. Chen R, Doolittle RF. gamma-gamma cross-linking sites in human and bovine fibrin. *Biochemistry* 1971;10(24):4487-4491.
3. Purves L, Purves M, Brandt W. Cleavage of fibrin-derived D-dimer into monomers by endopeptidase from puff adder venom (*Bitis arietans*) acting at cross-linked sites of the gamma-chain. Sequence of carboxy-terminal cyanogen bromide gamma-chain fragments. *Biochemistry* 1987;26(15):4640-4646.
4. Cottrell BA, Strong DD, Watt KW, Doolittle RF. Amino acid sequence studies on the alpha chain of human fibrinogen. Exact location of cross-linking acceptor sites. *Biochemistry* 1979;18(24):5405-5410.
5. Matsuka YV, Medved LV, Migliorini MM, Ingham KC. Factor XIIIa-catalyzed cross-linking of recombinant alpha C fragments of human fibrinogen. *Biochemistry* 1996;35(18):5810-5816.
6. Sobel JH, Gawinowicz MA. Identification of the alpha chain lysine donor sites involved in factor XIIIa fibrin cross-linking. *J Biol Chem* 1996;271(32):19288-19297.
7. Mockros LF, Roberts WW, Lorand L. Viscoelastic properties of ligation-inhibited fibrin clots. *Biophys Chem* 1974;2(2):164-169.
8. Shen L, Lorand L. Contribution of fibrin stabilization to clot strength. Supplementation of factor XIII-deficient plasma with the purified zymogen. *J Clin Invest* 1983;71(5):1336-1341.
9. Ryan EA, Mockros LF, Stern AM, Lorand L. Influence of a natural and a synthetic inhibitor of factor XIIIa on fibrin clot rheology. *Biophys J* 1999;77(5):2827-2836.
10. Ryan EA, Mockros LF, Weisel JW, Lorand L. Structural origins of fibrin clot rheology. *Biophys J* 1999;77(5):2813-2826.
11. Ariens RA, Philippou H, Nagaswami C, Weisel JW, Lane DA, Grant PJ. The factor XIII V34L polymorphism accelerates thrombin activation of factor XIII and affects cross-linked fibrin structure. *Blood* 2000;96(3):988-995.
12. Undas A, Ariens RA. Fibrin clot structure and function: a role in the pathophysiology of arterial and venous thromboembolic diseases. *Arterioscler Thromb Vasc Biol* 2011;31(12):e88-e99.

13. Standeven KF, Carter AM, Grant PJ, Weisel JW, Chernysh I, Masova L, Lord ST, Ariens RA. Functional analysis of fibrin gamma-chain cross-linking by activated factor XIII: determination of a cross-linking pattern that maximizes clot stiffness. *Blood* 2007;110(3):902-907.
14. Lord ST, Strickland E, Jayjock E. Strategy for recombinant multichain protein synthesis: fibrinogen B beta-chain variants as thrombin substrates. *Biochemistry* 1996;35(7):2342-2348.
15. Takebe M, Soe G, Kohno I, Sugo T, Matsuda M. Calcium ion-dependent monoclonal antibody against human fibrinogen: preparation, characterization, and application to fibrinogen purification. *Thromb Haemost* 1995;73(4):662-667.
16. Weisel JW, Nagaswami C. Computer modeling of fibrin polymerization kinetics correlated with electron microscope and turbidity observations: clot structure and assembly are kinetically controlled. *Biophys J* 1992;63(1):111-128.
17. Abou-Saleh RH, Connell SD, Harrand R, Ajjan RA, Mosesson MW, Smith DA, Grant PJ, Ariens RA. Nanoscale probing reveals that reduced stiffness of clots from fibrinogen lacking 42 N-terminal Bbeta-chain residues is due to the formation of abnormal oligomers. *Biophys J* 2009;96(6):2415-2427.
18. Allan P, Uitte de Willige S, Abou-Saleh RH, Connell SD, Ariens RA. Evidence that fibrinogen gamma' directly interferes with protofibril growth: implications for fibrin structure and clot stiffness. *J Thromb Haemost* 2012;10(6):1072-1080.
19. Evans RM, Tassieri M, Auhl D, Waigh TA. Direct conversion of rheological compliance measurements into storage and loss moduli. *Phys Rev E Stat Nonlin Soft Matter Phys* 2009;80(1):012501.
20. Shen LL, McDonagh RP, McDonagh J, Hermans J, Jr. Fibrin gel structure: influence of calcium and covalent cross-linking on the elasticity. *Biochem Biophys Res Commun* 1974;56(3):793-798.
21. Spraggon G, Everse SJ, Doolittle RF. Crystal structures of fragment D from human fibrinogen and its crosslinked counterpart from fibrin. *Nature* 1997;389(6650):455-462.
22. Collet JP, Moen JL, Veklich YI, Gorkun OV, Lord ST, Montalescot G, Weisel JW. The alphaC domains of fibrinogen affect the structure of the fibrin clot, its physical properties, and its susceptibility to fibrinolysis. *Blood* 2005;106(12):3824-3830.
23. Chernysh IN, Nagaswami C, Purohit PK, Weisel JW. Fibrin clots are equilibrium polymers that can be remodelled without proteolytic digestion. *Sci Rep* 2012;2:879.

24. Mosesson MW. Fibrinogen and fibrin structure and functions. *J Thromb Haemost* 2005;3(8):1894-1904.
25. Carlisle CR, Sparks EA, Der LC, Guthold M. Strength and failure of fibrin fiber branchpoints. *J Thromb Haemost* 2010;8(5):1135-1138.
26. Francis CW, Marder VJ. Increased resistance to plasmin degradation of fibrin with highly crosslinked alpha-polymer chains formed at high factor XIII concentrations. *Blood* 1988;71(9):1361-1365.
27. Fraser SR, Booth NA, Mutch NJ. The antifibrinolytic function of factor XIII is exclusively expressed through alpha(2)-antiplasmin cross-linking. *Blood* 2011;117(23):6371-6374.
28. Helms CC, Ariens RA, Uitte de WS, Standeven KF, Guthold M. alpha-alpha cross-links increase fibrin fiber elasticity and stiffness. *Biophys J* 2012;102(1):168-175.

**Table 1: Summary of the effects of fibrin  $\alpha$ - and  $\gamma$ - chain cross-linking by FXIIIa on clot formation and structure.** All data are from this study, except the role of  $\gamma$ -chain cross-linking in increased stiffness<sup>13,26</sup>.

	$\alpha$ -chain	$\gamma$ -chain
<b>Fiber thickness over time</b>	↑	
<b>Fiber density</b>		↑
<b>Clot stiffness</b>	↑↑	↑ <sup>13,26</sup>
<b>Fibrin clot lysis rate</b>	↓	
<b>Fiber appearance time</b>	↓	
<b>Fiber tautness</b>	↑	

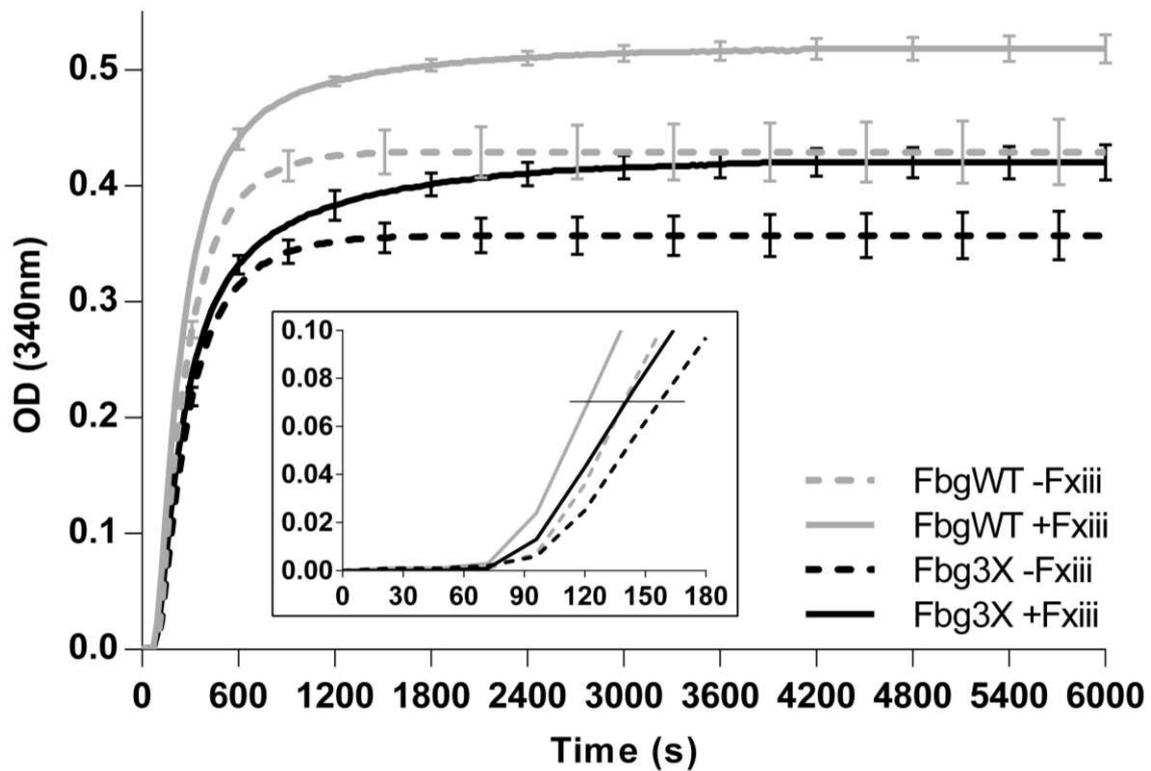


**Figure 1: Turbidity analysis of polymerizing clots produced with WT and 3X fibrinogen, in the absence or presence of factor XIII.** WT (grey line) and 3X (black line) fibrinogen at 0.5mg/mL were incubated with either TBS (dotted line) or 3.7  $\mu$ g/mL FXIII (plain line), in the presence of 0.1U/mL thrombin and 5mM CaCl<sub>2</sub>. Insert shows a scale up representation of the early stages of polymerization, with an arbitrary threshold used for comparison to confocal microscopy data. Error bars represent standard error of the mean.

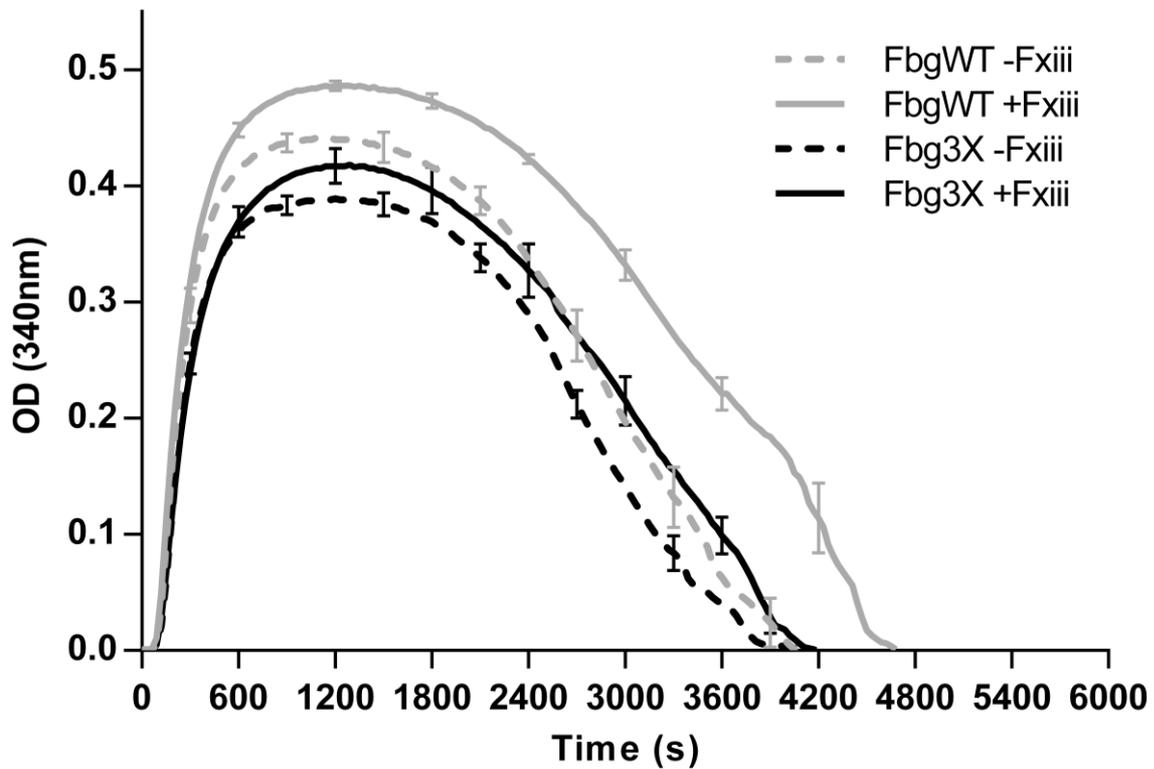


**Figure 2: Turbidity analysis of polymerizing and lysing clots produced with WT and 3X fibrinogen, in the absence or presence of FXIII.** WT (grey line) and 3X (black line) fibrinogen at 0.5mg/mL were incubated with either TBS (dotted line) or 3.7 $\mu$ g/mL FXIII (plain line), in the presence of 0.1U/mL thrombin and 5mM CaCl<sub>2</sub>, 100pM tPA, and 0.24 $\mu$ M Glu-plasminogen. Lysis rate was determined as  $\Delta$ OD/s at the steepest part of the curve. Error bars represent standard error of the mean.

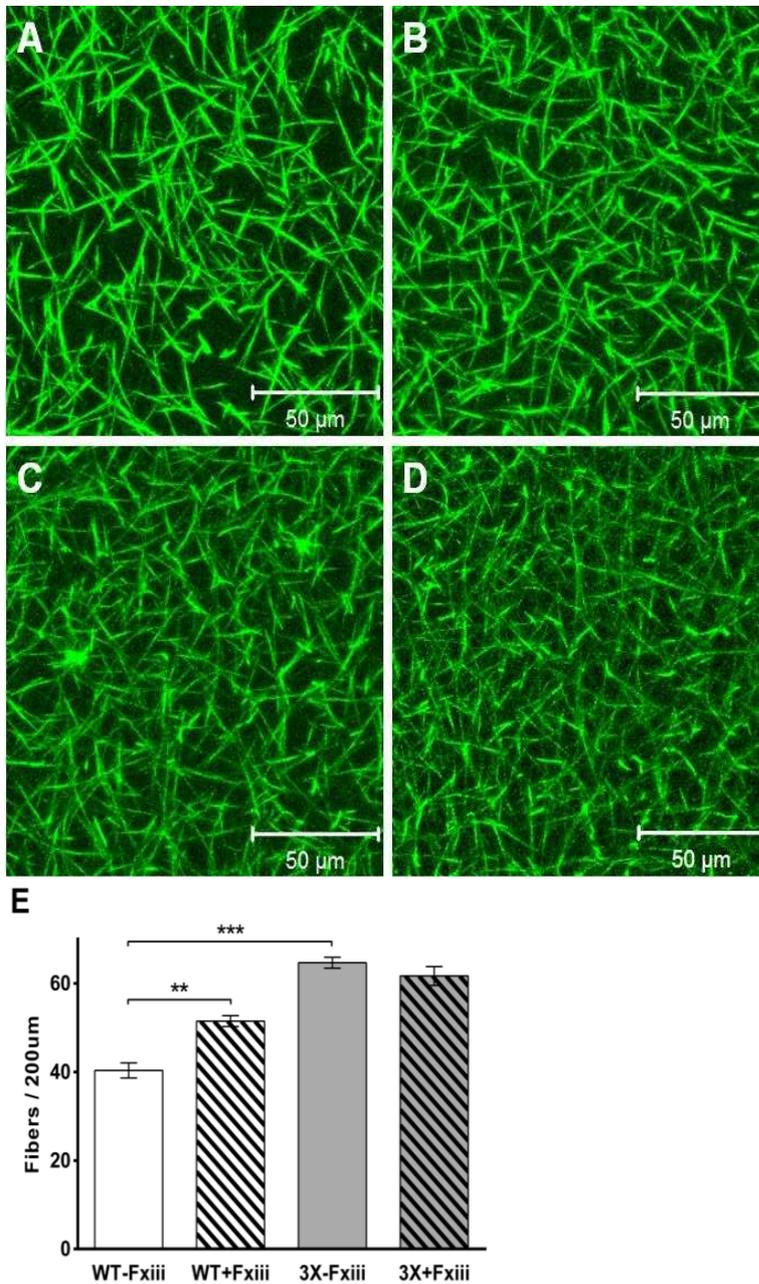


**Figure 3: Laser scanning confocal microscopy images of clots produced with WT and 3X fibrinogen, in the absence or presence of FXIII.** WT (upper panels) and 3X (lower panels) fibrinogen at 0.5mg/mL were incubated with either TBS (A, C) or 3.7μg/mL FXIII (B, D), in the presence of 1% AlexaFluor-labeled fibrinogen, 0.1U/mL thrombin and 5mM CaCl<sub>2</sub>. Pictures were taken after 60min incubation. Optical z-stacks (every 2μm over 20μm) were combined into single projected images. The scale bars indicate 50μm. Fiber density (E) was determined by counting the number of fibers crossing a section of 200μm long, in triplicate. Error bars represent standard error of the mean. \*\* p<0.01, \*\*\* p<0.005.

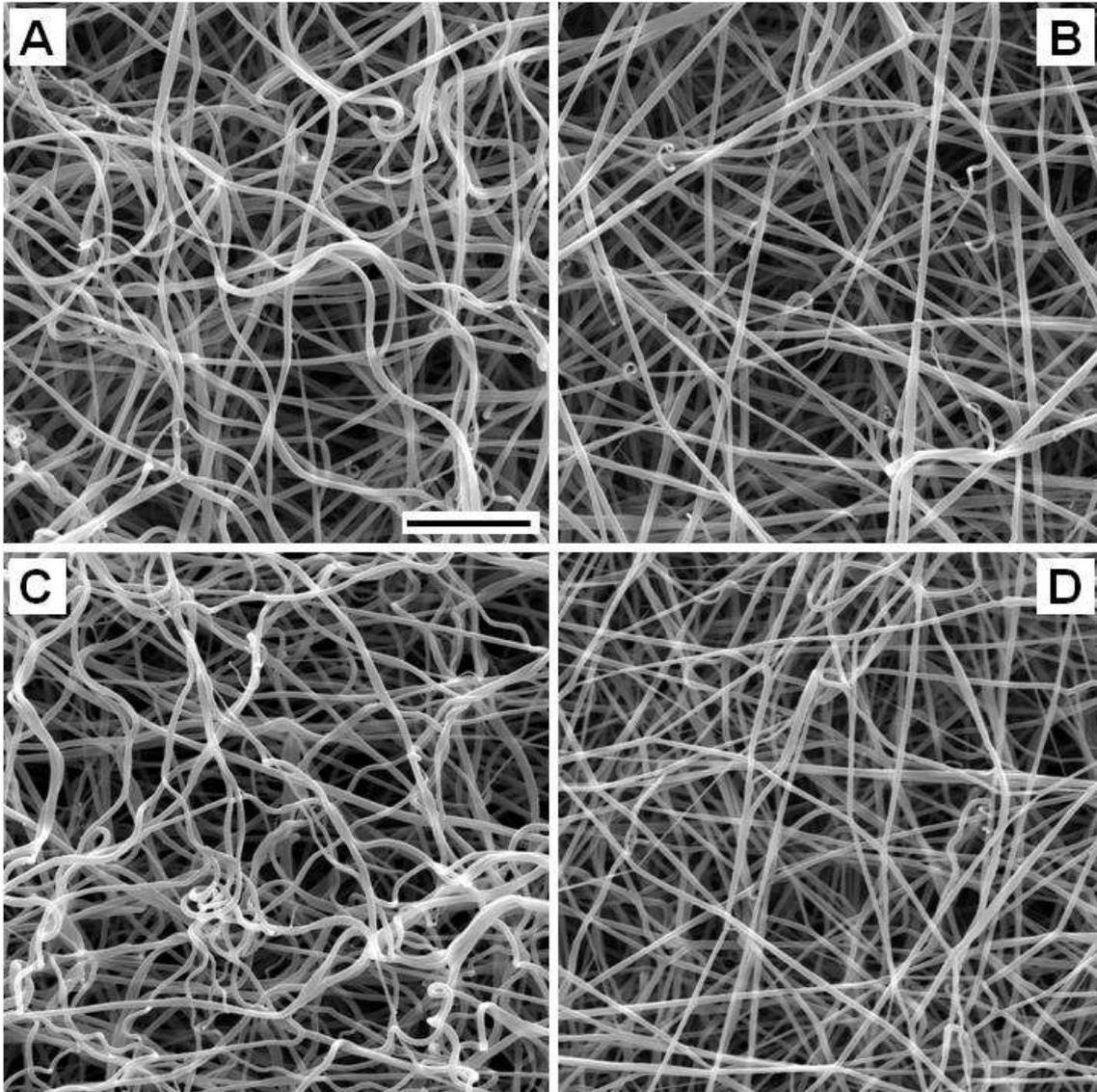


**Figure 4: Field emission scanning electron microscopy images of clots produced with WT and 3X fibrinogen, in the absence or presence of FXIII.** WT (upper panels) and 3X (lower panels) fibrinogen at 0.5mg/mL were incubated with either TBS (A, C) or 3.7 $\mu$ g/mL FXIII (B, D), in the presence of 0.1U/mL thrombin and 5mM CaCl<sub>2</sub>. The scale bar represents 2.5 $\mu$ m.

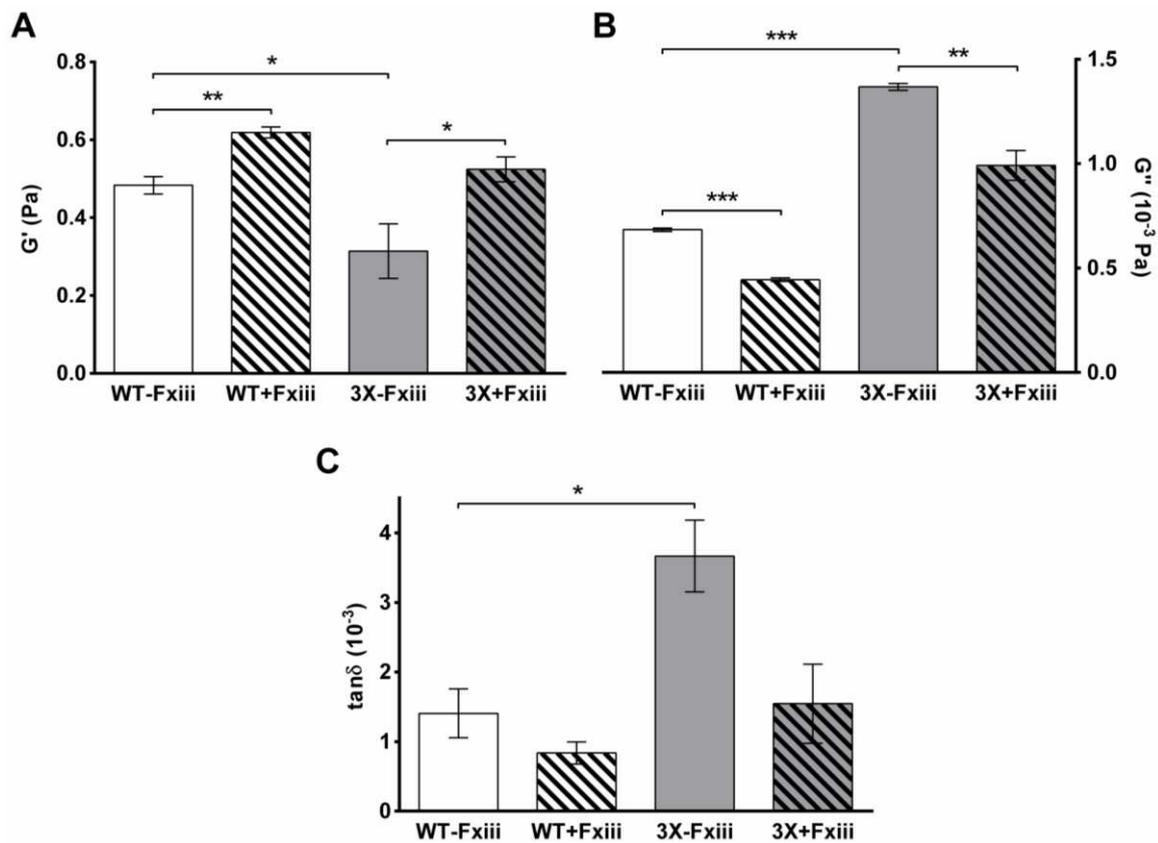


**Figure 5: Magnetic microrheometer measurements of clots produced with WT and 3X fibrinogen, in the absence or presence of FXIII.** WT and 3X fibrinogen at 0.5mg/mL were incubated with either TBS or 3.7 $\mu$ g/mL FXIII, in the presence of 0.1U/mL thrombin and 5mM CaCl<sub>2</sub>. A: Clot stiffness ( $G'$ ) measurements. B: Clot viscosity ( $G''$ ) measurements. C: Clot stability ( $\tan\delta$ ) measurements. Error bars represent standard error of the mean. \*  $p < 0.05$ , \*\*  $p < 0.01$ , \*\*\*  $p < 0.005$ .